Master's Thesis
석사 학위논문

Exploitation of Wireless Control Link in the Software-Defined LEO Satellite Network

Woncheol Cho (조 원 철 趙 原 澈)

Department of Information and Communication Engineering

DGIST

2020

Master's Thesis
석사 학위논문

Exploitation of Wireless Control Link in the Software-Defined LEO Satellite Network

Woncheol Cho (조 원 철 趙 原 澈)

Department of Information and Communication Engineering

DGIST

2020

Exploitation of Wireless Control Link in the Software-Defined LEO Satellite Network

Advisor: Professor Jihwan Choi
Co-advisor: Professor Sungjin Lee

by

Woncheol Cho
Department of Information and Communication Engineering
DGIST

A thesis submitted to the faculty of DGIST in partial fulfillment of the requirements for the degree of Master of Science in the Department of Information & Communication Engineering. The study was conducted in accordance with Code of Research Ethics[1]

12. 31. 2019

Approved by

Professor Jihwan Choi (signature)
(Advisor)

Professor Sungjin Lee (signature)
(Co-Advisor)

[1] Declaration of Ethical Conduct in Research: I, as a graduate student of DGIST, hereby declare that I have not committed any acts that may damage the credibility of my research. These include, but are not limited to: falsification, thesis written by someone else, distortion of research findings or plagiarism. I affirm that my thesis contains honest conclusions based on my own careful research under the guidance of my thesis advisor.

Exploitation of Wireless Control Link in the Software-Defined LEO Satellite Network

Woncheol Cho

Accepted in partial fulfillment of the requirements for the degree of Master of Science.

11. 14. 2019

Head of Committee	Prof. Jihwan Choi (signature)
Committee Member	Prof. Sungjin Lee (signature)
Committee Member	Prof. Kyung-Joon Park (signature)

MS/IC
201852016

조 원 철. Woncheol Cho. Exploitation of wireless control link in the software-defined LEO satellite network, 2020. Department of Information & Communication Engineering. 2020. 53p. Advisor: Prof. Jihwan Choi, Co-Advisor: Prof. Sungjin Lee

ABSTRACT

The low earth orbit (LEO) satellite network can benefit from software-defined networking (SDN) by lightening forwarding devices and improving service diversity. In order to apply SDN into the network, however, reliable SDN control links should be associated from satellite gateways to satellites, with the wireless and mobile properties of the network taken into account. Since these characteristics affect both control link association and gateway power allocation, we define this new cross layer problem as an SDN control link problem. The problem is discussed from the viewpoint of multilayers such as automatic repeat request (ARQ) and gateway power allocation at the Link layer, and split transmit control protocol (TCP) and link scheduling at the Transport layer. A centralized SDN control framework constrained by maximum total power is introduced to enhance gateway power efficiency for control link setup. Based on the power control analysis of the problem, a power-efficient control link algorithm is developed, which establishes low latency control links with reduced power consumption. Along with the sensitivity analysis of the proposed control link algorithm, numerical results demonstrate low latency and high reliability of control links established by the algorithm, ultimately suggesting the feasibility, both technical and economical, of the software-defined LEO satellite network.

Keywords: Software-defined satellite network, control link, cross layer optimization, power-efficient control link algorithm

CONTENTS

List of Figures

List of Tables

1 . INTRODUCTION

1.1 Software-Defined Satellite Network

Satellite networks have an advantage of global coverage and play a role as wireless backhaul for terrestrial communication networks even when the ground infrastructure is destroyed due to disasters. Despite these distinct strengths the main applications of satellite networks have been restricted to telephony or TV broadcasting, and network functionalities have been generally placed on ground hubs where most decisions on data routing are conducted on behalf of satellites. However, the extension of satellite service diversity over the last few decades is now heading to the provisioning of global Internet services through low earth orbit (LEO) satellite networks. Furthermore, the cost-competitive CubeSat network has been recently researched as a platform of the large-scale Internet of Things (IoT) [1]. As the satellite services rapidly catch up with terrestrial counterparts, network functionalities over satellite networks have been actively researched [2]-[4]. Main streams of research works can be divided into two promising concepts: Onboard processing (OBP) satellites which decide data forwarding and packet routing on the payload, and software-defined networking (SDN) which manages the control plane of the satellite network in the software-defined manner.

Owing to the advancement of application-specific integrated circuits (ASIC) and central processing units (CPU), OBP satellites are expected to conduct routing and scheduling decisions on the sky [2]. OBP satellites avoid unnecessary round-trip delays between satellites and ground hubs, thus reducing latency for control message establishment. They, however, require high computation power on the payload, which results in an increase in weight and complexity. Although these burdens are not a big problem for geosynchronous earth orbit (GEO) satellites, they can be a critical influence on survival of LEO satellites, especially for CubeSats [5]. In order to simultaneously meet the payload limitation of the LEO satellite and provide the network functionality on the satellite, SDN is one of the appropriate

candidates for the LEO satellite, with simple and light forwarding devices enabled by SDN [6].

Through the placement of virtual network functions (VNFs) such as deep packet inspection (DPI) or load balancing [7], the software-defined satellite network, previously introduced in [4], [8], can provide services which require diverse quality-of-service (QoS). The LEO satellite network with short propagation delays less than 10 ms is expected to support these diverse QoS requirements. Unlike the traditional network, the propagation delay between the controller and forwarding device also affects the latency for establishment of the packet handling rules in SDN [9]. Especially in case of event handling reactive to emergency situations such as traffic congestion or link cessation, large latency is fatal to the network performance. Prior to the packet forwarding or event handling, round-trip propagation delays of GEO satellites, as high as 250 ms, are not suitable for the software-defined satellite network which is anticipated as the platform of diverse services. Instead, as the characteristics of GEO and LEO satellites are taken into account, GEO satellites are expected to be backhauls for the software-defined LEO satellite network for satellite application services.

Traditional communication networks implements both control and data planes in the same purpose-built network devices, which results in inflexibility and high CAPEX/OPEX for upcoming data demand for the 5G applications [6], [10], [11]. SDN has been promised as an approach to overcome the problems of existing ossified networks. Its main features compared to those of conventional networks are as follows [6], [12], [13]: The control plane is logically centralized while the data plane is physically distributed. The SDN controller provides packet handling rules to forwarding devices based on the abstract network view through the open southbound application programming interface (API). The abstract network view enables the management plane to simply manage network reconfigurations or to facilitate introduction of new abstraction.

An architecture for the software-defined LEO satellite network is delineated in Fig. 1. Software-defined satellites serve user equipment through 5G new radio (NR) gNodeBs (gNBs), home-equipped gateways, or directly. A hub consists of a satellite gateway, a network control center (NCC), a network

management center (NMC), and a performance-enhancing proxy (PEP). NCC and NMC manage the terrestrial-satellite network through control plane functions and management plane functions respectively [14]. PEP improves end-to-end performances of the whole network by splitting ground wired links and lossy gateway-satellite links (GSLs). Satellites and switches on the backbone network are software-defined, and routing/scheduling decisions are conducted on the ground SDN controller located in the backbone network. Along with the decision functionality, the SDN controller establishes control links from the controller to all the satellites.

However, weather attenuation at high frequencies beyond Ku and Ka-bands can be severe, which impinges on the reliability of the control links. Table 1 indicates the frequency band application with the federal communications commission (FCC) of five companies. Since the frequency band beyond Ku and Ka-bands have not been actively employed, several commercial enterprises have applied the bands to the FCC for the purpose of the future satellite services.

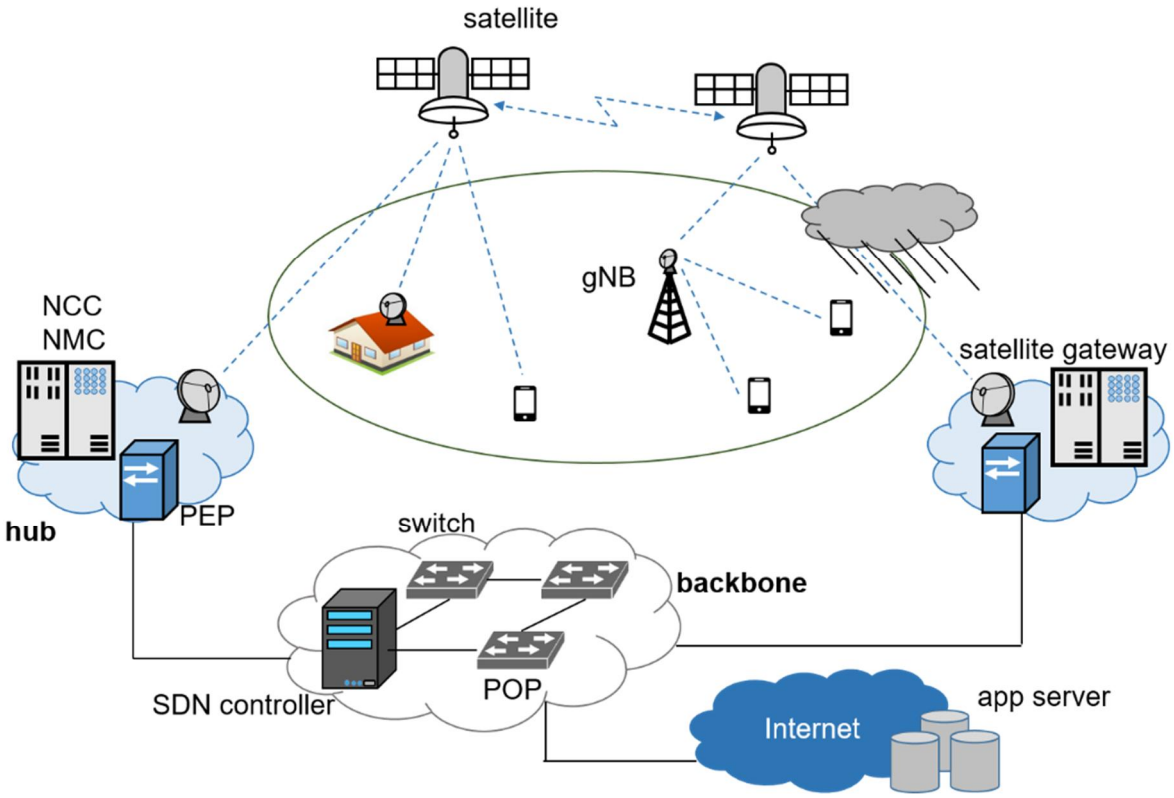

Figure 1. An architecture for the software-defined LEO satellite network.

To adopt SDN to the future satellite environment, accordingly, reliable control links should be associated from the SDN controller to all the satellites, taking the extreme wireless characteristics of the LEO network into account.

1.2 Wireless SDN Control Link Problem Statement

Regardless of proactive or reactive SDN modes, average latency minimization of control link setup is the foremost objective of the controller [3], [9]. The control messages with rules of forwarding and routing should be transmitted to each node before data packets arrive at the node. Therefore, the control link latency can have a critical influence on the latency of data transmission, which is directly related to QoS. Given that a control message generally has a small packet size and is prioritized over data, time-varying propagation delay and control link reliability dominantly impinge on the link latency. Link reliability can be represented as an outage probability dependent on the gateway power, explained further in Section 2.2.1. The gateway power is generally high in the software-defined satellite network owing to the frequent update of control messages and extreme weather attenuation and fading. Further discussion will be held in Section 2.3.2. Although maximum power allocation can achieve full reliability, power efficiency of gateways has become increasingly important for the sake of network greenness [15]-[17]. In addition, gateways are generally located at power-limited remote areas where power control is of great importance. The gateway power allocation and the control link association are closely related with the channel environment, which should be optimized in a coupled manner. We define this

TABLE 1. FREQUENCY BAND APPLICATION WITH THE FCC OF EACH COMPANY.

Enterprise	Frequency band
SpaceX	Ku/Ka/V
OneWeb	Ku/V
Telesat	Ka/V
O3b Networks	Ku/Ka/V
Theia Holdings	Ka/V

cross layer problem as a wireless SDN control link problem which is analyzed from the viewpoint of multilayers such as automatic repeat request (ARQ) and gateway power allocation at the Link layer, and split transmit control protocol (TCP) and link scheduling at the Transport layer.

1.3 Contributions and Overview of Thesis

The cross layer control link problem in the software-defined satellite network minimizes the expected latency that is the function of propagation delay and gateway power. To fully comprehend the expected latency, we explore the latency from the Transport layer to the Link layer in a top-down approach in Section 2. A logically centralized control framework constrained by a maximum total power P_{ctrl} is elaborated, followed by the SDN control link problem formulation.

Based on the solid analysis of the SDN control link problem, we propose a power-efficient control link algorithm in Section 3 which establishes low latency control links while reducing power consumption of link setup. Since the control link problem is prohibitive in computational complexity due to combinatorial link association, a sub-optimal link algorithm with polynomial complexity is proposed. Through the numerical results of the proposed control link algorithm in Section 4, we analyze the feasibility from the perspective of latency and reliability. This approach additionally lays a cornerstone for a general wireless SDN control link problem of applying SDN into a network of flying objects, such as satellites, unmanned aerial vehicles (UAVs) and high altitude platforms (HAPs).

Furthermore, it will be shown that latency and reliability of control links established by the proposed control link algorithm are directly affected by a maximum total power P_{ctrl}. To fully exploit the power efficiency of the proposed algorithm, we analyze the local sensitivity and stability of the algorithm with respect to P_{ctrl}. Perturbation analysis and latency observation present an appropriate value of P_{ctrl} above a point of diminishing return, which simultaneously provides low latency and high reliability. Section 5 concludes the paper and presents future work.

1.4 Related Works

Traditionally, as the LEO satellite network functions as a backbone, there have been several studies to adopt connection-oriented asynchronous transfer mode (ATM) or multi-protocol label switching (MPLS) protocols into the LEO satellite network [18], [19], which are widely exploited in a core cloud of the terrestrial network. Especially, in [19], a control framework of the MPLS-based satellite network is proposed and the importance of a centralized control station is emphasized. The author in [20] demonstrated the network routing concept in the ATM-based satellite network with inter-satellite links (ISLs).

In recent years, there have been many research outcomes attempting to adapt the control framework of the satellite network to SDN. The authors in [4] applied various concepts such as VNF, software-defined radio (SDR) and SDN to the satellite network, and constructed a scenario of the software-defined satellite network. Its advantages such as integration of terrestrial and satellite networks are introduced in [21]. In [14], the reliability of the satellite backhaul is introduced as along with the advantages of SDN. However, the wireless control link is not explained in detail and the paper lacks the consideration on viability of implementing SDN on the satellite. The authors in [22] proposed a control framework where the physically distributed controllers are mounted on LEO satellites, called control satellites. While ISLs guarantee reliable connections between control and data satellites, the extra cost of link state synchronization between control satellites are required in comparison with fixed ground SDN controllers. Other research work has focused on the performance analysis of adopting SDN to the LEO satellite network [23]-[25]. A couple of papers proposed congestion avoidance or traffic engineering algorithms based on SDN and achieved better performance over the existing LEO satellite network [23], [24]. The authors in [25] proposed throughput improvement for the steady state and the handover state exploiting SDN.

We demonstrate the feasibility of the software-defined satellite network by proposing a control link algorithm dependent on wireless environments. Unlike our approach here, most of previous studies have addressed the controller placement problem to resolve how to apply SDN into large scale networks

[9], [26], [27]. In [9], the SDN controller placement problem was first proposed, which presented the feasibility of adopting SDN into the large scale network. In the satellite network, dynamic control satellite placement in the LEO satellite network was addressed in [28], and joint placement of controllers and satellite gateways in the software-defined satellite-terrestrial network was solved in [3]. These papers, however, did not take wireless channels and power allocation into account.

2 . MODELING AND FORMULATION

2.1 Control Link Association

2.1.1 Graph Model

The topology of the software-defined satellite network is depicted in Fig. 2. For the control plane, ground SDN controllers manage a set of satellite gateways $\mathbf{W} = \{g_1, g_2, \dots, g_M\}$ and software-defined LEO satellites $\mathbf{S} = \{s_1, s_2, \dots, s_N\}$, where M and N are the number of gateways and satellites, respectively. Controllers gather channel state information (CSI) of the network and compose the abstract network view. There are more satellites around the world than gateways in general ($M < N$). Controllers are physically distributed all over the world to cover the global satellite network. In order to retain the logically centralized control plane, controllers share network knowledge through the open east/westbound API [6].

An example control link is associated between a controller and satellite s through gateway g as a

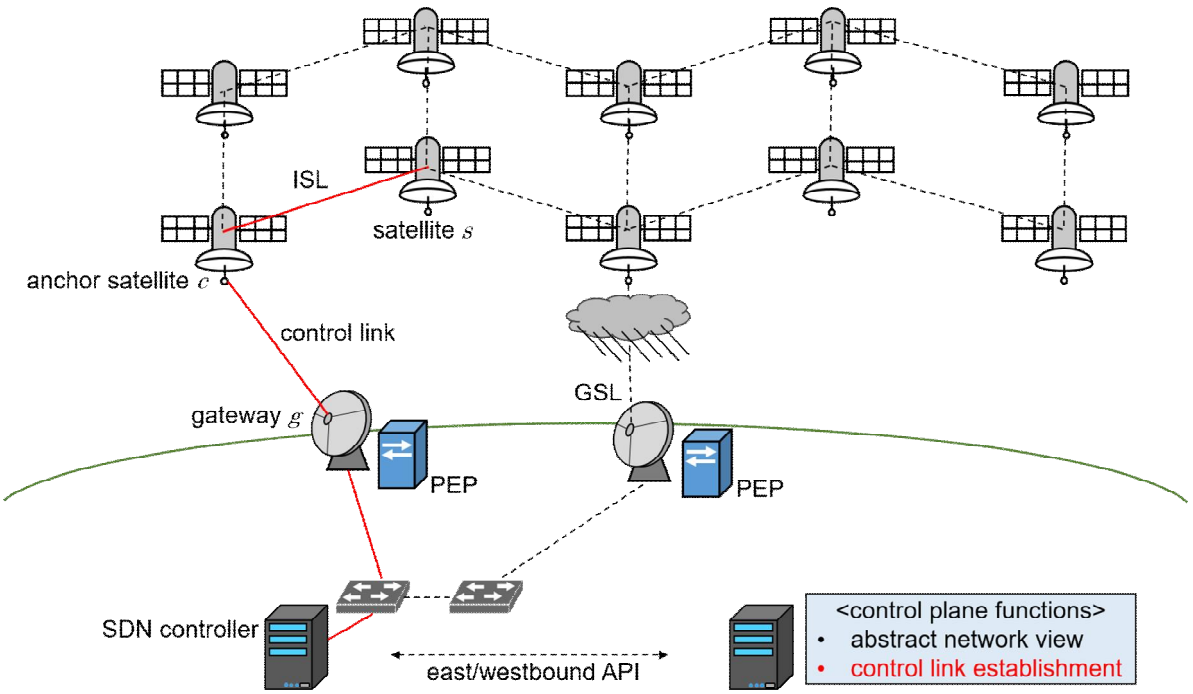

Figure 2. Topology of the software-defined LEO satellite network and control link establishment.

red solid line in Fig. 2. In the example, the controller associates the link with the shortest path, while avoiding unreliable channels suffering from weather attenuation. Since M is smaller than N and gateways are not always inside the footprint of each satellite, several satellites should receive control messages from the same satellites through ISL. These satellites play a role of the anchor points in the network [29], and we call them anchor satellites (denoted as c in Fig. 2). The control link has possibly multiple hops through the controller, a gateway, an anchor satellite, and ISL if necessary.

The GSL, whose lossy channel characteristics impinge on transmit control protocol (TCP) connection, is separated from the ground wired link at the Transport layer by the PEP located at a hub. We represent the terrestrial-satellite network as a graph $G(V, E)$, with vertices $V = \mathbf{S} \cup \mathbf{W}$ and edges E which consists of GSLs and ISLs, except for ground wired links. Note that the control link should be established from the controller to each satellite $s \in \mathbf{S}$, over which control messages toward satellite s are transmitted.

2.1.2 ARQ and Split TCP

SDN employs connection-oriented TCP establishment [30]. For a reliable connection of the control link, especially a connection via GSL, the automatic repeat request (ARQ) protocol controls errors based on retransmissions. The transmitter (gateway) retransmits a control message to the receiver (satellite) if the gateway receives a negative acknowledgement (NACK) or does not receive any feedback within an elapsed time (round-trip propagation delay in this paper without loss of generality). The transmitter waits for a round-trip propagation delay, thus a control message setup time under condition of no retransmission equals the round-trip propagation delay of the control link. Here transmission and queueing delays are negligible compared to propagation delays, since a control message generally has a small packet size and is prioritized over data.

The end-to-end control link from the controller to satellite s is concatenated with ground wired links and wireless satellite links (including GSL and ISL) at the Transport layer. ISL, meanwhile, is

only affected by the propagation distance, owing to a good channel condition at the altitude above 200 km. In this case, wireless satellite links can be split into lossy GSL and reliable ISL by onboard proxy satellite [31]. Figure 3 illustrates the control message flows of (a) standard TCP connection and (b) split TCP connection by onboard proxy satellite, under condition of no retransmission. The solid line indicates control message flow, the dotted line indicates end-to-end TCP ACK, and the dashed line indicates local ACK (LACK). When the onboard proxy satellite receives the message it sends LACK to the gateway, and transmit the message to satellite s through ISL. For the end-to-end semantics of TCP establishment, satellite s lastly sends ACK to the gateway [32]. We formulate the control link latency considering both practical TCP connection models. As discussed later in Section 2.2.2, each model has its pros and cons.

2.1.3 Link Association Variable

We introduce an indicator variable $x_{ij}^{(s)} \in \{0,1\}$ which is 1 when edge $\{i,j\} \in E$ is a part of the control link for satellite s. If satellite s is a destination of a control message, it can be described with the indicator variables as

$$\sum_{i:\{i,s\}\in E} x_{is}^{(s)} - \sum_{i':\{s,i'\}\in E} x_{si'}^{(s)} = 1. \quad (1)$$

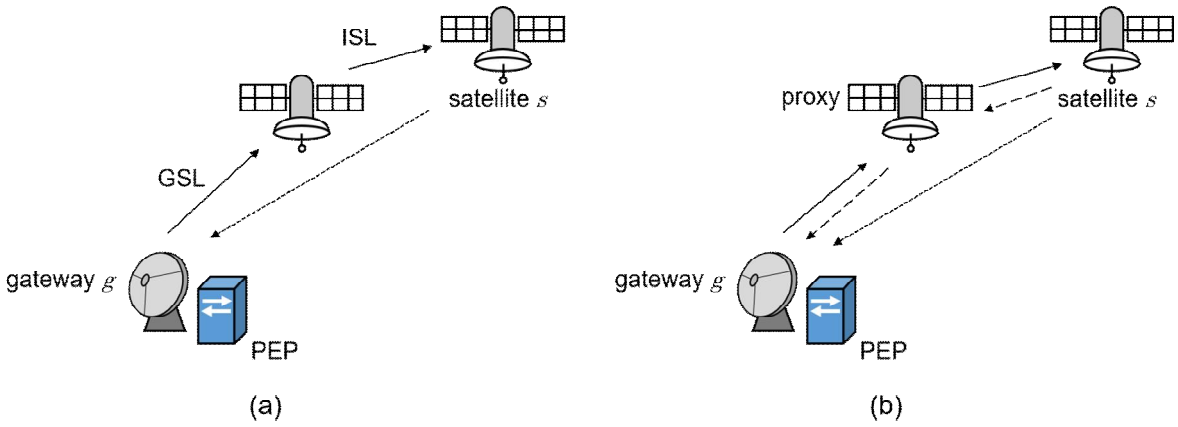

Figure 3. Control message flows of (a) standard TCP connection and (b) split TCP connection.

Given a control message toward satellite s that satisfies Eq. (1) and gateway $g \in \mathbf{W}$ from which the control message originates, the control message setup time d_{gs} from g to s can be formulated as:

$$d_{gs} = \sum_{\{i,j\} \in E} x_{ij}^{(s)} d_{ij}, \tag{2}$$

where d_{ij} is a round-trip propagation delay of edge $\{i,j\}$. Note that the selection of gateway g is dependent on the indicator variable $x_{ij}^{(s)}$, which can be represented as $\sum_{i:\{g,i\} \in E} x_{gi}^{(s)} = 1$. In the case of split TCP connection enabled by onboard proxy satellite, the control message setup time d_{gs}^{split} toward s can be formulated as:

$$d_{gs}^{\text{split}} = \sum_{g \in \mathbf{W}} \sum_{i:\{g,i\} \in E} x_{gi}^{(s)} d_{gi} + \sum_{\{i,j\} \in E, i \notin \mathbf{W}} x_{ij}^{(s)} d_{ij} + \sum_{\{i',j'\} \in E} x_{i'j'}^{(s)} \cdot \frac{d_{i'j'}}{2}, \tag{3}$$

where the first two terms denote the control message flow and LACK through GSL and ISL, and the last term is the delay for the final end-to-end ACK transmission. We assume that the propagation distance does not change during the time the control message transmits, thus the end-to-end ACK propagation delay is half of the round-trip propagation delay.

Each satellite gateway has a tracking antenna, enabling a GSL between the anchor satellite and the gateway for a time slot, which is described as

$$\sum_{g \in \mathbf{W}} \sum_{i:\{g,i\} \in E} x_{gi}^{(s)} = 1. \tag{4}$$

Additionally, given gateway set $\mathbf{W}$ and satellite s, data flow between intermediate vertices should be conserved under the constraint given as

$$\sum_{j:\{i,j\}\in E} x_{ij}^{(s)} - \sum_{j':\{j',i\}\in E} x_{j'i}^{(s)} = 0, \qquad \forall i \notin \{s\} \cup \mathbf{W}. \tag{5}$$

2.2 Control Link Reliability and Expected Latency Formulation

2.2.1 Control Link Reliability and Gateway Power

Control link reliability can be represented as an outage probability. When control links are established, link outages should be avoided because they incur retransmissions with redundant power consumption and latency increase. We suppose that the controllers, managing the global-scale network topology, have large-scale channel knowledge of ISL and GSL, which mainly consists of weather attenuation and path loss. Under the condition of line-of-sight (LOS) between gateways and satellites, GSL is modeled to follow small-scale Nakagami fading [33], and the knowledge of channel distribution is available only to the controllers. The shape factor $m = 1$ implies that the channel suffers Rayleigh fading and m gradually increases as the strength of the specular scattered signal increases compared to diffuse scattering. ISL is only affected by the propagation distance, owing to a good channel condition at the altitude above 200 km. The connection causing the control link outage toward s is the GSL between gateway g such that $\sum_{i:\{g,i\}\in E} x_{gi}^{(s)} = 1$ and anchor satellite c such that $x_{gc}^{(s)} = 1$. Anchor satellite c sometimes is identical to satellite s, depending on the topology of the satellite network. The link outage probability between g and c has the closed form as below [34]:

$$P_{gc}^{out} = 1 - \frac{\Gamma\left(m, \frac{m\gamma_{th}}{\overline{\gamma_{gc}}}\right)}{\Gamma(m)}, \tag{6}$$

where γ_{th} is the signal-to-noise ratio (SNR) threshold required for receiving a control message, and $\overline{\gamma_{gc}}$ is the average received SNR at anchor satellite c. $\Gamma(m)$ is the gamma function and $\Gamma\left(m, \frac{m\gamma_{th}}{\overline{\gamma_{gc}}}\right)$ is the upper incomplete gamma function [35, Eq.(6.5.3)]. The average SNR $\overline{\gamma_{gc}}$ is written as:

$$\overline{\gamma_{gc}} = \frac{H_{gc} P_g}{W N_0}, \tag{7}$$

where H_{gc} and P_g are the large-scale channel gain and the transmit power from gateway g to anchor satellite c, respectively, W is the uplink bandwidth, and N_0 is the noise power density. Large-scale channel gain $H_{gc} = \alpha_g \cdot l_{gc}$ consists of free space path loss l_{gc} and weather attenuation α_g. Path loss l_{gc} is modelled as $l_{gc} = \left(\frac{\sqrt{G_{gc}} f}{2\pi d_{gc}}\right)^2$ [36], where G_{gc} is the product of antenna field radiation patterns of gateway g and anchor satellite c, f is the carrier frequency, and d_{gc} is the round-trip propagation delay between gateway g and anchor satellite c.

2.2.2 Expected Latency Formulation

We define the number of transmissions N_{gc} for control message setup from gateway g to anchor satellite c caused by outages under the condition of $P_g > 0$ ($N_{gc} = 0$ for $P_g = 0$). Since LEO satellites move at high speeds along orbits, channels between gateways and satellites suffer from fast small-scale fading, i.e. coherence time T_c is much less than the propagation delay. For instance, assume that the LEO satellite at altitude 1,400 km employs a frequency band with carrier frequency 18 GHz (near Ku-band). Since the satellite moves at speed 7.16 km/s to keep the orbit, Doppler shift D equals to 0.43 MHz. Coherence time $T_c \approx 1/(4D)$ [37] for ease of calculation, and coherence time T_c equals to 0.58 μs. Considering the propagation delay in the order of ms, coherence time is much less than the propagation delay. Accordingly, each transmission trial is reasonably assumed to be an independent and identically distributed (i.i.d.) Bernoulli random variable with success probability $1 - P_{gc}^{out}$. Thus, the number of transmissions N_{gc} follows geometric distribution [38], whose ensemble average $\mathbb{E}[N_{gc}]$ is given as

$$\mathbb{E}[N_{gc}] = \frac{1}{1 - P_{gc}^{out}} = \frac{\Gamma(m)}{\Gamma\left(m, \frac{m\gamma_{th}}{\overline{\gamma_{gc}}}\right)}, \tag{8}$$

With control message setup delay d_{gc} represented as Eq. (2) under the standard TCP and the average number of transmissions as Eq. (8), the expected steady-state latency L_{gs} of control message establishment from g to s is expressed as

$$L_{gs} = \sum_{\{i,j\} \in E} x_{ij}^{(s)} d_{ij}\, \mathbb{E}[N_{gc}], \tag{9}$$

which is a function of indicator variables $x_{ij}^{(s)}$ and gateway transmit power P_g. On the other hand, for the split TCP connection, the outage caused by the GSL leads to retransmission only in GSL, but not in ISL. We assume that the final end-to-end ACK transmission is not disturbed by the channel unreliability due to the small size of ACK packet. Then, the expected latency L_{gs}^{split} of the split TCP connection can be formulated as

$$L_{gs}^{\text{split}} = \sum_{g \in \mathbf{W}} \mathbb{E}[N_{gc}] \sum_{i:\{g,i\} \in E} x_{gi}^{(s)} d_{gi} + \sum_{\{i,j\} \in E, i \notin \mathbf{W}} x_{ij}^{(s)} d_{ij} + \sum_{\{i',j'\} \in E} x_{i'j'}^{(s)} \cdot \frac{d_{i'j'}}{2}, \tag{10}$$

where $\mathbb{E}[N_{gc}] \geq 1$ for $P_g > 0$, and $\mathbb{E}[N_{gc}] = 0$ for $P_g = 0$. Note that non-zero power incurs at least one transmission.

The expected latency L_{gs} is convex with respect to transmit power P_g, under the condition that the shape factor m is an integer with the proof given in Appendix. In the same way, L_{gs}^{split} also holds convexity with respect to transmit power P_g, of which the proof is omitted for conciseness. Fig. 4 presents the expected latencies of the standard TCP and split TCP connections as a function of transmit power by changing the shape factor and weather attenuation. Obviously, under harsh weather conditions,

the split TCP connection indicates lower expected latency by splitting outage-prone GSL and reliable ISL. Under mild weather conditions, meanwhile, the split TCP protocol provides larger expected latency since the onboard proxy satellite additionally transmits LACK and end-to-end TCP ACK transmission which is represented in Eq. (3) (cf. Eq. (2)).

Under harsh weather attenuation and for both TCP connections, the lowest expected latency of Rayleigh fading (i.e. $m = 1$) is achievable in the low transmit power region, since the well-scattered signals

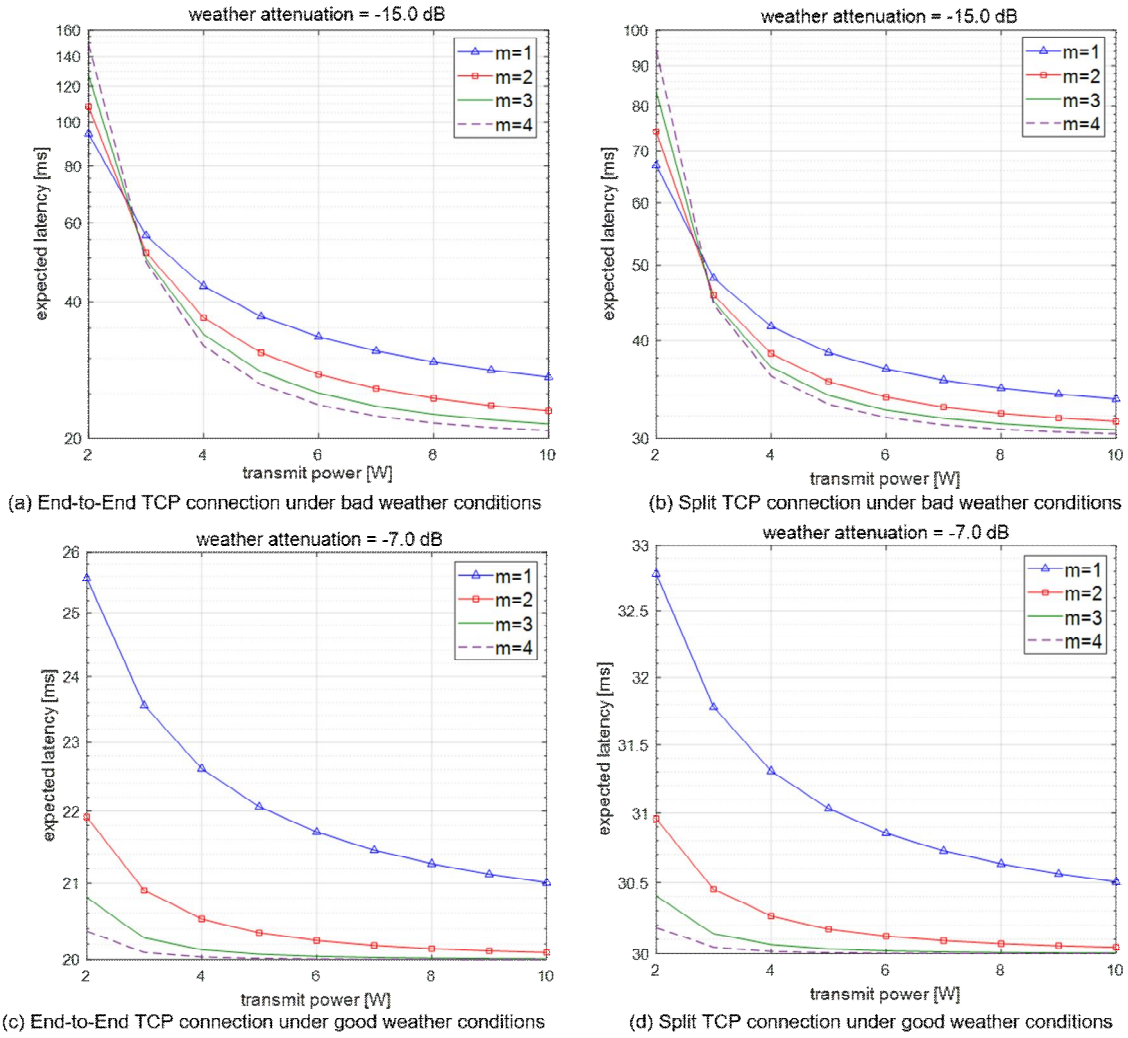

Figure 4. Expected latencies of the two TCP connections by changing transmit power under the condition of different weather attenuation and round-trip propagation delay 20 ms, including ISL transmissions.

can prevent outages. As the shape factor m increases (i.e. the specular scattered signal strength increases), additional power transmission greatly reduces the expected latency. Since satellite gateways are usually located where the shape factor is high (i.e. free from obstructions), large marginal returns of the expected latency in the low power region are a crucial factor to efficiently reduce gateway power consumption. Since the expected latency with both the TCP connections display a similar tendency with respect to transmit power, we employ L_{gs} with the standard end-to-end TCP connection as a typical metric of the expected latency and formulate the SDN control link problems.

2.3 SDN Control Link Problem

2.3.1 Expected Latency Minimization Problem

The optimization variables are gateway transmit power P_g and indicator variables $x_{ij}^{(s)}$. The primary objective of the controller is to minimize the expected latency. The expected latency minimization problem for each satellite s is formulated as:

$$\underset{P_g, x_{ij}^{(s)}}{\text{minimize}} \quad L_{gs} \tag{11}$$

$$\text{subject to} \quad P_g \leq P_{GW,g}, \quad \forall g \in \mathbf{W}, \tag{12}$$

$$(1), (4), (5),$$

where $P_{GW,g}$ is the maximum power amount available for gateway g. In general, this cross layer optimization problem has prohibitive complexity owing to combinatorial link association. Through the power control analysis, however, this can be reduced to a control link association problem with on/off power allocation due to its characteristic of full power allocation, as derived in the following. The optimization problem holds strong duality with respect to power P_g with Slater's condition satisfied [39]. Then, the optimal solution derived by the Karush-Kuhn-Tucker (KKT) condition is also the primal

optimal. Applying the KKT condition, given a feasible control link association variable $x_{ij}^{(s)}$, the optimum power allocated for each gateway g is obtained by the following equation:

$$\left.\frac{\partial L_{gs}}{\partial P_g}\right|_{P_g=P_g^*} = -d_{gs}\cdot\frac{\Gamma(m)}{P_g}\cdot\left\{\frac{1}{\Gamma\left(m,\frac{m\gamma_{th}}{\overline{\gamma_{gc}}}\right)}\right\}^2\cdot\left(\frac{m\gamma_{th}}{\overline{\gamma_{gc}}}\right)^m\cdot e^{-\frac{m\gamma_{th}}{\overline{\gamma_{gc}}}}$$
$$= -\lambda_g \tag{13}$$

where λ_g is a Lagrangian multiplier associated with the gateway power constraint in Eq. (12). If the optimum transmit power P_g^* is non-zero, implying that $\sum_{i:\{g,i\}\in E} x_{gi}^{(s)} = 1$, then the derivative $\left.\frac{\partial L_{gs}}{\partial P_g}\right|_{P_g=P_g^*}$ is always negative. Thus, the Lagrangian multiplier λ_g is larger than zero, followed by the optimal power $P_g^* = \mathrm{P}_{GW,g}$ by the complementary slackness [39]. Another possible value of P_g^* is zero, where gateway g is not exploited in the given control link ($\sum_{i:\{g,i\}\in E} x_{gi}^{(s)} = 0$). This full power allocation property holds for the optimal control link represented with $x_{ij}^{(s)*}$ since the property always holds for every feasible link. As a result, we conclude that the expected latency minimization problem is reduced into the link association problem with on/off gateway transmit power allocation ($P_g^* = 0$ or $\mathrm{P}_{GW,g}$). The result shows that gateways are allocated with a sufficient power margin to ensure reliability.

2.3.2 Power-Efficient SDN Control Link Problem

Regardless of the constellation that the LEO satellite network is designed with, the links between satellites and ground gateways or user equipments always change over time. Even the data with a same origin and a destination can be transmitted by different satellites if the service time differs. Hence, flow tables should be updated according to the time-varying network. Furthermore, as dynamic network slicing, which can be highly facilitated by SDN [40], [41], is implemented in a near future, control updates

will increase drastically. Given that the link connection between gateways and LEO satellites is about 10 minutes, it is necessary to frequently transmit and update control information. In addition, Section 4 will show that a large amount of power is required to ensure high reliability since the reliability of the control link is largely affected by rain attenuation and fading of the satellite channel. Accordingly, the amount of power consumed for control link setup is generally large. Although it is proven in Section 2.3.1 that the sufficient power margin maximizes reliability, allocating full power leads to power inefficiency incompatible with the perspective of green communication [16]. Furthermore, since gateways are located at power-limited remote areas in general, power efficiency at gateways is one of the most significant factors to realize the software-defined satellite network.

In order to maintain low latency control links while saving power, the controller should exploit the diminishing marginal return of expected latency with respect to power in a cross layer approach. In Fig. 4 (a), we demonstrate high marginal returns of the expected latency in the low transmit power region under the harsh weather condition, in particular with the large shape factor m. For instance, the expected latency L_{gs} decreases to about 17 ms if P_g increases from 3 to 4 W, while it decreases to less than 1 ms if P_g increases from 7 to 8 W with $m = 4$. In order to exploit large marginal returns in the low power region, a logically centralized SDN control framework is exploited to moderate power consumption for control link setup by introducing the maximum total power, and we formulate the power-efficient SDN control link problem given as

$$\underset{P_g, x_{ij}^{(s)}}{\text{minimize}} \quad \frac{1}{N} \sum_{g \in \mathbf{W}} \sum_{s \in \mathbf{S}} L_{gs} \tag{14}$$

$$\text{subject to} \quad P_g \leq P_{GW}, \qquad \forall g \in \mathbf{W}, \tag{15}$$

$$\sum_{g \in \mathbf{W}} P_g \leq P_{ctrl}, \tag{16}$$

$$(1), (4), (5), \qquad \forall s \in \mathbf{S},$$

where P_{ctrl} is the maximum total power required for control link setup, which directly affects both power consumption and latencies of SDN control links. The maximum total power P_{ctrl} is established by the management plane. In general, the per-node average latency, same as Eq. (14), is set as an objective function in the controller placement problem [3], [26], which minimizes the average latency by searching the optimal placement of controllers. On the other hand, the proposed SDN control link problem seeks the optimal link association $x_{ij}^{(s)*}$ and power allocation P_g^* jointly.

The power-efficient control link problem holds strong duality with respect to power P_g with Slater condition satisfied. Then the optimal solution derived by the KKT condition is also the primal optimal. Applying the KKT condition, given feasible control link association variable $x_{ij}^{(s)}$, the optimally allocated power of each gateway g is obtained by solving the equation given as

$$\frac{1}{N}\frac{\partial L_{gs}}{\partial P_g}\bigg|_{P_g=P_g^*} + \lambda_g = -\Lambda < 0, \tag{17}$$

where λ_g and Λ are Lagrangian multipliers associated with the gateway power constraint in Eq. (15) and the maximum amount of the total power in Eq. (16), respectively. Gateway power allocation can be divided into two cases: either 1) $P_g^* = P_{GW}$ $(\lambda_g \geq 0)$, where the transmit power of gateway g is at the maximum value, or 2) $P_k^* < P_{GW}$ $(\lambda_k = 0)$, where the transmit power of gateway k is not saturated. Then the following inequality holds:

$$\frac{\partial L_{gs}}{\partial P_g}\bigg|_{P_g=P_g^*} \leq \frac{\partial L_{ks}}{\partial P_k}\bigg|_{P_k=P_k^*} = -N\Lambda < 0, \tag{18}$$

where $P_k^* < P_g^* = P_{GW}$. Due to the convexity of expected latency L_{gs} with respect to transmit power, the derivative in inequality (18) becomes larger as the amount of power increases under the condition of fixed weather attenuation and round-trip propagation delay. However, owing to the different weather conditions of gateways and various propagation delays for each satellite, inequality (18) holds for power allocation $P_k^* < P_g^*$. The impact of weather attenuation and round-trip propagation delay d_{gs} on the derivative of the expected latency is depicted in Fig. 5, with gateway power P_g fixed at a certain amount P_0 (e.g. 5 W in Fig. 5). The z-axis represents the derivative with respect to the allocated power, $\left.\frac{\partial L_{gs}}{\partial P_g}\right|_{P_g=P_0}$. As the gateway suffers from much severe weather attenuation or longer round-trip propagation delay between g and s, $\left.\frac{\partial L_{gs}}{\partial P_g}\right|_{P_g=P_0}$ decreases. Then inequality (18) denotes that, given an associated control link represented with $x_{ij}^{(s)}$, a large amount of power should be allocated to the satellite

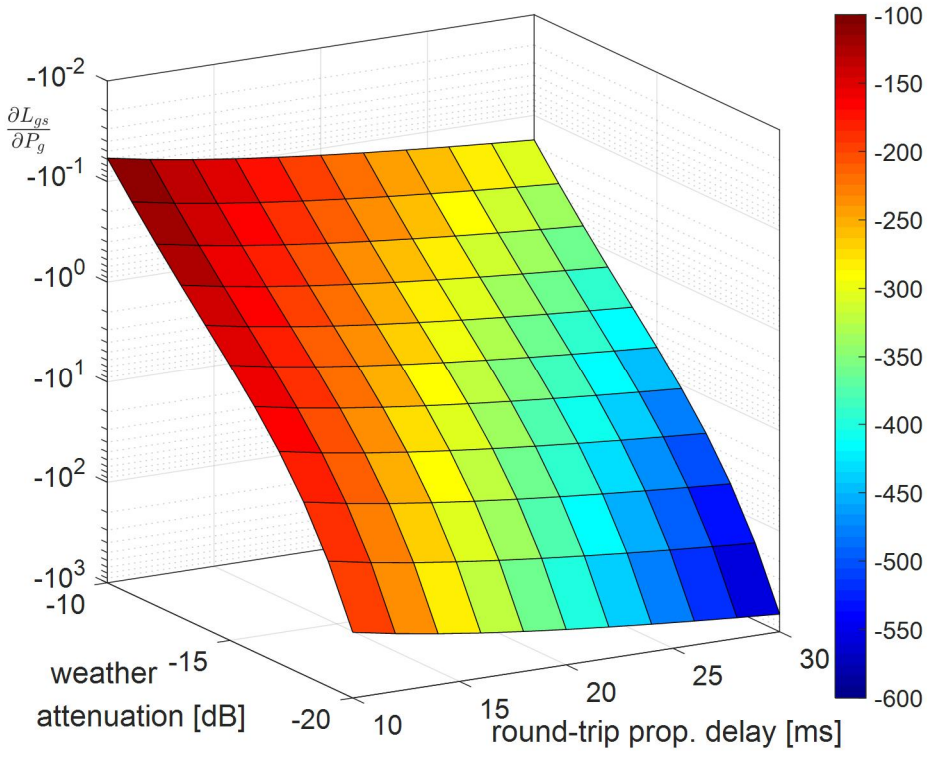

Figure 5. The derivative $\left.\frac{\partial L_{gs}}{\partial P_g}\right|_{P_g=P_0}$ by changing weather attenuation and round-trip propagation delay.

in severe weather attenuation or at a long distance. The satellites served by gateways under severe weather attenuation are allocated more power because they are prone to outages. Repetitive outages result in control performance degradation in the whole network. The satellites at a longer distance are also allocated more power since the latency caused by retransmissions is much larger than the satellites at a shorter distance. Especially, the derivative decreases rapidly as weather attenuation worsens, indicating that weather attenuation increases power consumption more than the long propagation delay.

The result can be interpreted from a viewpoint of link association which is coupled with the power allocation problem. Through the power control analysis, given the link association, much power is allocated to the satellite with lower $\left.\frac{\partial L_{gs}}{\partial P_g}\right|_{P_g=P_0}$. On the other hand, under fixed power allocation, links with larger $\left.\frac{\partial L_{gs}}{\partial P_g}\right|_{P_g=P_0}$ should be associated to reduce power consumption since a large value of the derivative is the necessary and sufficient condition for saving power allocation. Hence, in order to minimize the average control link latency while reducing power allocation, the optimally associated link is with large $\left.\frac{\partial L_{gs}}{\partial P_g}\right|_{P_g=P_0}$ by avoiding association with a gateway suffering from a severe weather condition and/or to a distant satellite as indicated in Fig. 5.

3 . SDN CONTROL LINK ALGORITHM

The controller requires the knowledge of round-trip propagation delay and weather attenuation of the whole network in order to calculate the average number of transmission $\mathbb{E}[N_{gc}]$ caused by outages. The path loss is predictable because the satellite constellation operates in a pre-determined way, and the knowledge of quasi-static weather attenuation, whose coherence time is longer than the control link latency in general, can be achieved by frequently probing channel states. Hence, periodic probing of weather conditions and path loss is sufficient for the controllers to be aware of d_{ij} and H_{gc}. For coherent network knowledge of SDN controllers, periodic synchronization is performed through open west/eastbound API. In addition, to respond rapidly to an event that causes network congestion or link cessation, satellites report the network problems to the control plane in real-time.

Based on the abstract network view, the control plane operates control link algorithms both in proactive (periodic) or reactive (event-triggered) manners. In the steady state, it is sufficient for SDN controllers to establish control links periodically. However, unpredictable link congestion and outages require new traffic engineering in real-time. Thus, the control link algorithm should establish low latency control links with low computational complexity to tackle events rapidly.

The power-efficient SDN control link problem searches all the feasible links to simultaneously solve link association and power allocation. A brute-force recursive algorithm (depth-first search (DFS) algorithm) to find all the feasible links between gateway g and satellite s has complexity in the order of $\mathcal{O}(N!)$, which makes the control plane difficult to operate in an event-triggered manner. We propose a sub-optimal algorithm that has polynomial complexity but guarantees low latency on this account. A key idea of the algorithm is that $\left.\frac{\partial L_{gs}}{\partial P_g}\right|_{P_g=P_0}$ acts as a hinge [2], [42], decoupling link association and power allocation. From the analysis of the power-efficient SDN control link problem in Section 2.3.2, the link with the largest $\left.\frac{\partial L_{gs}}{\partial P_g}\right|_{P_g=P_0}$ is selected as an optimal control link for each s.

As demonstrated in Fig. 5, weather attenuation has a worse impact on the derivative than propagation delay. Note that a link associated with enough power is mainly affected by propagation delay with the small outage probability, while a link with small gateway power is heavily affected by weather attenuation. Based on these observations, for every satellite $s \in \mathbf{S}$, the controller establishes a control link with small power P_{small} which is expected to have a large value of $\frac{\partial L_{gs}}{\partial P_g}\Big|_{P_g=P_0}$. Following the link association represented by $x_{ij}^{(s)}$ for all s, the power-efficient control link problem is reduced into the power allocation problem given as:

$$\begin{aligned} \underset{P_g}{\text{minimize}} \quad & \frac{1}{N}\sum_{g\in\mathbf{W}}\sum_{s\in\mathbf{S}} L_{gs} \\ \text{subject to} \quad & (15), (16). \end{aligned} \tag{19}$$

The proposed sub-optimal SDN control link algorithm is described in Algorithm 1. The link association procedure exploits the shortest path algorithm Shortest_Path() where the input is the round-trip propagation delay weighted by an average number of transmissions, for all $g \in \mathbf{W}$ and all $s \in \mathbf{S}$ to establish control link $x_{ij}^{(g\to s)}$ from g to s. Given that the computation complexity of the simple Dijkstra algorithm as a shortest path algorithm is $\mathcal{O}(N^2)$, the total complexity of the link association procedure is $\mathcal{O}(MN^3)$, where M is the number of gateways and N is that of satellites, respectively. The power allocation procedure employs the barrier method, which optimizes the inequality-constrained convex problem, to solve the reduced power allocation problem. For example, if we can approximate the expected latency L_{gs} with respect to power P_g as a quadratic function, as seen in Fig. 4 (a), the third derivative of the objective function (19) can be upper-bounded by the constant value. This makes the objective function self-concordant [43], which gives the complexity of the barrier

method within the order $\mathcal{O}\left(\sqrt{M}\log\left(\frac{M}{t^{(0)}\epsilon}\right)\right)$, where $t^{(0)}$ is an initial value of the approximation accuracy parameter and ϵ is a tolerance [39]. In summary, the total computation complexity of the proposed control link algorithm is given by

$$\mathcal{O}\left(MN^3+\sqrt{M}\log\left(\frac{M}{t^{(0)}\epsilon}\right)\right)=\mathcal{O}(MN^3), \tag{20}$$

which is mainly dependent on the link association procedure.

Algorithm 1 : Power-efficient SDN control link algorithm.

Data: H_{gc}, d_{ij}
Result: $P_g, x_{ij}^{(s)}$
begin
  Initialize P_{small}.
  for *all* $s \in \mathbf{S}$ **do**
    for *all* $g \in \mathbf{W}$ **do**
      $P_g := P_{small}$.
      $\mathbb{E}[N_{gc}] := \Gamma(m)/\Gamma\left(m, \frac{m\gamma_{th}WN_0}{H_{gc}P_g}\right)$.
      $cost := d_{ij}\mathbb{E}[N_{gc}]$.
      $x_{ij}^{(g\to s)} := \text{Shortest\_Path}(cost)$.
    end
    $x_{ij}^{(s)} := \min_{g\in\mathbf{W}} x_{ij}^{(g\to s)}$.
  end
  Initialize P_g, $\mu > 1$, tolerance ϵ, and parameter $t^{(0)}$.
  $t := t^{(0)}$.
  while $(M+1)/t > \epsilon$ **do**
    $P_g^*(t) := \text{argmin}_{P_g}\left\{\frac{t}{N}\sum_s L_{gs} - \phi\right\}$, $\phi = \sum_g \log(P_{GW,g} - P_g) + \log(P_{ctrl} - \sum_g P_g)$.
    $P_g := P_g^*(t)$.
    $t := \mu t$.
  end
end

4 . NUMERICAL RESULTS AND ANALYSIS

The proposed power-efficient link algorithm is applied to the LEO satellite network for numerical evaluation. We adopt the Walker delta constellation as the LEO satellite constellation and the detail parameters are referred to as the Celestri constellation [44], [45]. The Walker delta constellation provides permanently maintainable ISLs with acceptable pointing, acquisition, and tracking requirements [19], [46]. However, the time-varying link between the gateway and the anchor satellite, and the resulting handover have a negative impact on the control link reliability. The handover will not be discussed in further detail, and details are referred to [25] which applied multipath TCP connections to solve the handover challenges. On the other hand, the Walker star constellation exploited in Iridium has a seam between counter-rotating planes, and the ISLs between inter-plane orbits change with time [18]. These drawbacks require much effort to obtain the same control link reliability as in the delta constellation.

The proposed algorithm can be analyzed in other satellite network constellations with diverse scales of satellites and gateways by the method presented in this section. As the number of satellites increases, the control link latency escalates, and thus more gateways and controllers should be deployed to solve this network scalability problem. The key issues of network scalability are an increment in CAPEX/OPEX due to the increase of gateways and controllers, and a maintenance cost of the coherent control plane through east/westbound API. An analysis for this can be one of further research topics.

Table 2 shows the LEO satellite constellation and communication parameters in the simulation. We set shape factor $m = 4$ because gateways are generally located in locations free from obstructions. Power constraints of all the gateways are assumed to be equal to 10 W without loss of generality. In the simulation, the weather condition follows the two-state Markov process where good and bad weather states are randomly selected every 30 minutes. Under a bad weather condition, the signals transmitted from the gateway are set to have weather attenuation of 13 dB more than under good weather. Satellite gateways are distributed according to the Globalstar gateway locations [47], indicated in Figure 6.

Full power link algorithms without/with CSI are compared with the proposed algorithm as benchmarks. Full power algorithm without CSI can be regarded as the control link algorithm employed in the existing software-defined wired network. On the other hand, it is shown in Section 2.3.1 that the expected latency minimization problem reduces to a link association problem with on/off power allocation. Accordingly, the full power link algorithm with CSI is equivalent with the optimal expected latency minimization (ELM) algorithm, which is named as the ELM algorithm in this section. The latency comparison with the non-SDN algorithm may be trivial and is not considered here, since SDN has a great advantage of being able to manage the whole network at a centralized control plane.

TABLE 2. SATELLITE CONSTELLATION AND COMMUNICATION PARAMETERS.

Satellite constellation	
No. of satellites	48
No. of planes	8
Orbit inclination	53
Altitude	1,400 km
ISL distance range	5,860 km
Communication parameters	
No. of gateways	27
Uplink distance range	1,800 km
Uplink bandwidth	0.5 GHz
Maximum power	10 W
Shape factor	4
Weather attenuation	-13.01 dB
SNR threshold	-10 dB
Noise power density	4.0×10^{-21} W/Hz

Figure 6. The distribution of satellite gateways.

4.1 Latency Analysis and Feasibility of the Software-Defined Satellite Network

Let δ_s denote the latency for control message establishment of satellite s averaged over 1,000 simulation iterations for the steady-state performance analysis. Retransmission events caused by outages are considered in the measured latency δ_s as a random variable following the outage probability. The metrics of our interest are the average of per-satellite latency $\mathbb{E}[\delta_s]$ and the maximum latency $\max \delta_s$ for every satellite $s \in \mathbf{S}$. Fig. 7 represents the average latency $\mathbb{E}[\delta_s]$ over all the satellites and provides the comprehensive network performance of the proposed algorithm. Maximum total power P_{ctrl} of the power-efficient algorithm is set at 50 W. The daily average of $\mathbb{E}[\delta_s]$ of the power-efficient algorithm is 41.01 ms, while those of ELM and the full power algorithm without CSI are 39.77 ms and 62.35 ms, respectively. The latency performance of the proposed algorithm is comparable with that of the ELM algorithm, only about 3% higher on average.

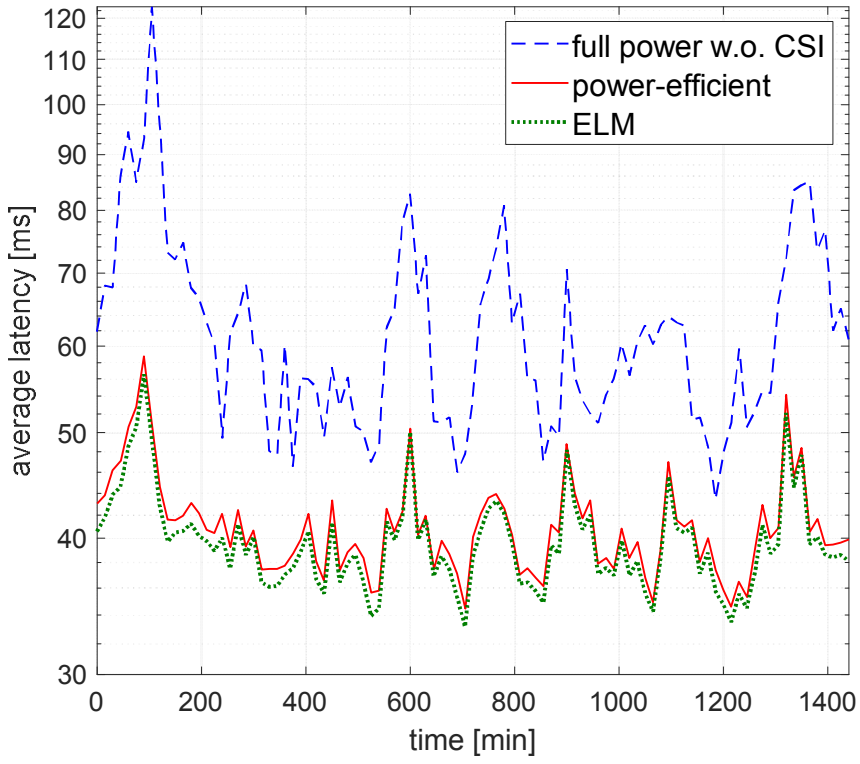

Figure 7. Average latency comparison between control link algorithms for 24 hours.

TABLE 3. COMPARISON BETWEEN CONTROL LINK ALGORITHMS.

Algorithm	ELM	Power-efficient
Gateway transmit power per satellite	10.77 W	6.40 W
Running time	13.54 ms	24.69 ms
Asymptotic complexity	$\mathcal{O}(MN^3)$	

Table 3 presents the comparison between ELM and the proposed algorithm with respect to gateway transmit power consumption per satellite, running time (both in simulation), and asymptotic complexity. The power-efficient algorithm utilizes maximum total power $P_{ctrl} = 50$ W. Both gateway transmit power consumption and running time are averaged over 100 simulation iterations. Since the control link problem optimizes power allocation in a time slot in the steady state, real power consumption is taken into account due to the control message transmission based on time division multiple access (TDMA) and/or retransmissions caused by outages. The proposed algorithm, which is the power-constrained version of ELM, markedly reduces the total power consumption for control link setup. Its average value of per-satellite power consumption is only 59% of the ELM algorithm. The cross layer approach of the proposed algorithm makes the best use of the diminishing marginal return of the expected latency efficiently, reducing power consumption while preserving average latency performance.

In addition, Table 3 compares running time and asymptotic computational complexity between the two algorithms. The simulation were performed in Matlab R2018a running on a PC with a 4.00 GHz CPU, 32.0 GB RAM, and Windows 10 OS. Since the ELM algorithm associates the control link by allocating full power $P_{GW,g}$ to minimize the expected latency, the complexity of the ELM algorithm is $\mathcal{O}(MN^3)$, which is same as the proposed algorithm. Simulation running time, however, shows a significant difference due to the power allocation procedure. While the analytical complexity of proposed algorithm is mainly dependent on the link association procedure, as derived in Eq. (20), the optimization parameters such as initial point $t^{(0)}$ and tolerance ϵ affect the practical running time in simulations. To sum up, the power-efficient control link algorithm efficiently reduces power consumption of the control framework at the cost of increased running time.

In Fig. 8, the maximum latency $\max \delta_s$ of each algorithm is compared. Maximum total power P_{ctrl} of the power-efficient algorithm is set at 50 W. The maximum latency $\max \delta_s$ indicates the latency of the last satellite in which the control message is established. Since data routing should operate after the establishment of the control message to all satellites, $\max \delta_s$ directly decides QoS requirements and finally becomes the bottleneck of the control link algorithm. Hence, from the perspective of implementation of SDN into the satellite network, the maximum latency can be more critical than the average latency. The maximum latencies of both ELM and the proposed algorithm are extremely lower than that of the control link algorithm without CSI. Interestingly, contrary to the average latency result, the daily average of $\max \delta_s$ of the proposed algorithm is 89.46 ms and that of ELM is 97.90 ms, about 9% higher.

The results in Fig. 8 also provide the feasibility of operating SDN for LEO satellites. As introduced in Section 1.4, there have been many prior studies on ATM-based LEO satellite networks [18], [20],

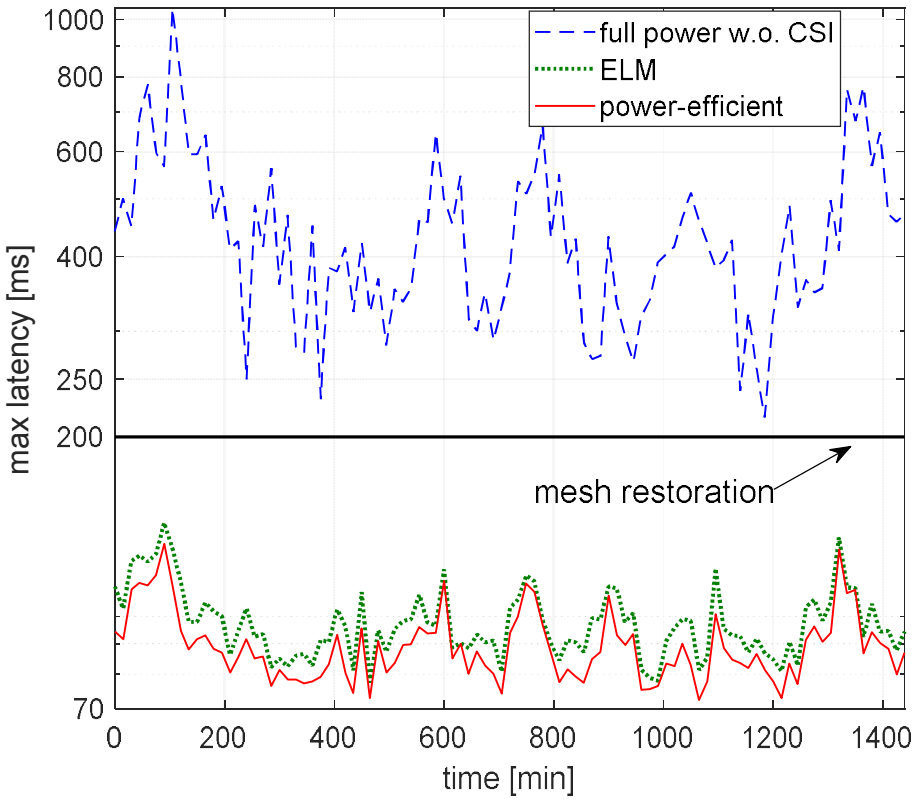

Figure 8. Maximum latency comparison between control link algorithms for 24 hours.

which have been deemed as the typical control framework of LEO satellite networks to the date. Accordingly, by comparing the maximum latency $\max \delta_s$ of the algorithms and the mesh restoration time of about 200-250 ms, which is the time duration when ATM circuit rerouting may be triggered [9], [48], it is sufficient to demonstrate the feasibility of applying SDN into the network. To strictly prove the feasibility, the network average latency from the ground controllers to gateways should be considered together. However, in order to figure out the terrestrial network latency, a comprehensive discussion on the network should be developed, such as the dynamic controller placement problem or the joint controller and gateway placement problem. This is beyond the scope of this paper. Fortunately, the latency analyses on Chinanet [3] and on Internet Topology Zoo [9] confirm that the average latency of China- and US-sized topologies is less than 10 ms. Therefore, if the latency of the satellite network satisfies the mesh restoration time with an enough margin, the latency of the entire network including the global terrestrial network is expected to satisfy the mesh restoration time.

The maximum latency $\max \delta_s$ of the full power control link algorithm without CSI always exceeds the mesh restoration time, suggesting that the control link algorithm employed in the wired terrestrial network cannot be applied into the LEO satellite network as it is. On the other hand, $\max \delta_s$ of the ELM and power-efficient algorithm are always much lower than the mesh restoration time. Consuming much less power on the control framework, the proposed algorithm always provides $\max \delta_s$ below the mesh restoration time. Even taking into consideration the latency of the terrestrial network from the controller to gateways, the maximum latency of the power-efficient control link algorithm satisfies the mesh restoration time sufficiently. Additionally, the management plane should select P_{ctrl} carefully, considering the trade-off between power consumption and the latency performance, which will be covered in Section 4.2.

To comprehend the result accurately, we analyze how each algorithm associates the control links. Fig. 9 and Fig. 10 represent the averages of per-satellite round-trip propagation delays and outage probabilities of control links established by the three control link algorithms, respectively. Results are averaged

over 1,000 iterations for the steady-state performance analysis and maximum total power P_{ctrl} is set at 50 W. First, the full power link algorithm without CSI associates control links with the shortest propagation delay without considering the outage probability. As a result, both average and maximum latency grow due to repetitive outages. Link reliability can be represented as an outage probability. From the perspective of reliability, the channel-ignorant algorithm (exploited in terrestrial SDN) is not applicable to the wireless network. On the contrary, both the power-efficient and ELM algorithms have the strategy to associate links with the minimum expected latency. The proposed algorithm, however, lacks the absolute power to reduce the outage probability of GSL where the gateway suffers from severe weather attenuation. Accordingly, the proposed algorithm detours to the gateway under a good weather condition, if possible, at the expense of longer propagation delay. On the other hand, the ELM algorithm aggressively exploits the outage probability if the expected latency of the link with transmission is lower than that of the detour without retransmission. Thus, although the per-satellite average latency of ELM is always lower than the power-efficient algorithm, the maximum latency of the proposed is lower than that of ELM where the satellite is served by the gateway with a relatively large outage probability.

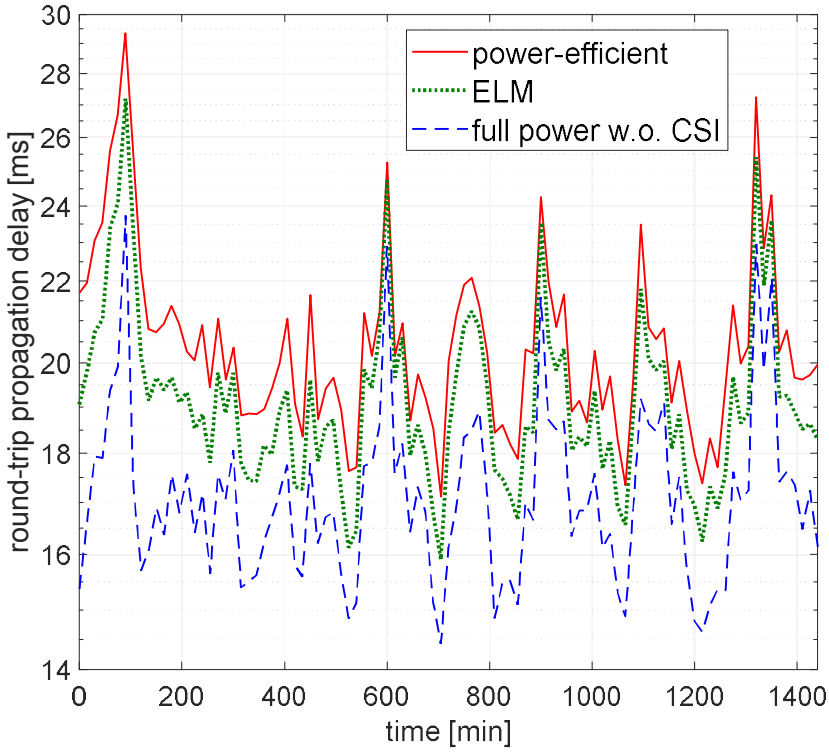

Figure 9. Average of round-trip propagation delay of control link algorithms for 24 hours.

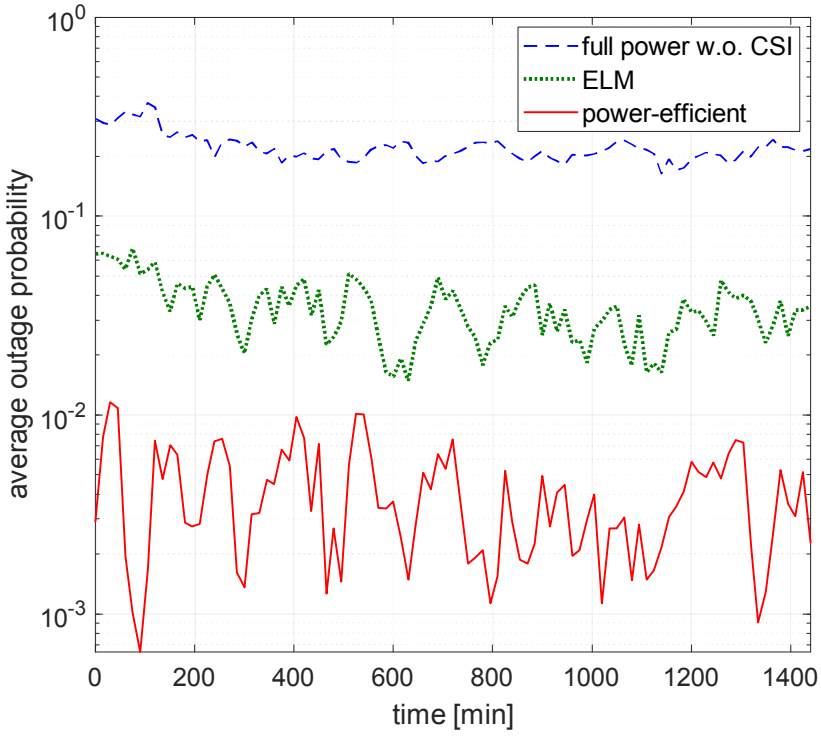

Figure 10. Average of per-satellite outage probability of control link algorithms for 24 hours.

4.2 Sensitivity Analysis and Selection of the Maximum Total Power

Maximum total power P_{ctrl} influences both the latency performance and power consumption. Small P_{ctrl} makes gateways consume less power for control link setup but the latency performance can be degraded exponentially. For a proper selection of P_{ctrl}, which is the most critical part of the proposed algorithm, we analyze the sensitivity and stability of the power-efficient control link algorithm through the perturbation [39] and latency analysis. Furthermore, we suggest a valid parameter selection method of P_{ctrl}, which takes advantage of a diminishing law of the marginal return of sensitivity or stability with respect to P_{ctrl}.

Local sensitivity is the metric to evaluate how sensitive the optimization problem is to the perturbing constraint. For the sensitivity analysis with respect to P_{ctrl}, we formulate a perturbed version of the power-efficient SDN control link problem as below:

$$\underset{P_g, x_{ij}^{(s)}}{\text{minimize}} \quad \frac{1}{N}\sum_{g\in\mathbf{W}}\sum_{s\in\mathbf{S}} L_{gs} \tag{21}$$

$$\text{subject to} \quad P_g \le P_{GW,g}, \quad \forall g \in \mathbf{W}, \tag{22}$$

$$\sum_{g\in\mathbf{W}} P_g - P_{ctrl} \le u, \tag{23}$$

$$(1), (4), (5), \quad \forall s \in \mathbf{S},$$

where u is a perturbing variable. When $u > 0$ the total power consumption is relaxed; otherwise the consumption is tightened. Let L^*_{avg} and $L^*_{\text{avg}}(u)$ be the optimal values of the power-efficient SDN control link problem and the perturbed problem, respectively. Then we have the following inequality which provides the lower bound of $L^*_{\text{avg}}(u)$:

$$L^*_{\text{avg}}(u) \ge L^*_{\text{avg}} - \Lambda u, \tag{24}$$

where Λ is a Lagrangian multiplier associated with the maximum amount of the total power. With perturbation relaxed for $u > 0$, the inequality (24) yields the following as $u \to 0$

$$\left.\frac{\partial L^*_{\text{avg}}(u)}{\partial u}\right|_{u=0} \geq -\Lambda. \tag{25}$$

While the opposite inequality holds for $u < 0$ with tightened perturbation, we can obtain the local sensitivity of the power-efficient control link problem with respect to P_{ctrl}:

$$\left.\frac{\partial L^*_{\text{avg}}(u)}{\partial u}\right|_{u=0} = -\Lambda. \tag{26}$$

Fig. 11 demonstrates the local sensitivity $\left.\frac{\partial L^*_{\text{avg}}(u)}{\partial u}\right|_{u=0}$ of the perturbed power-efficient SDN control

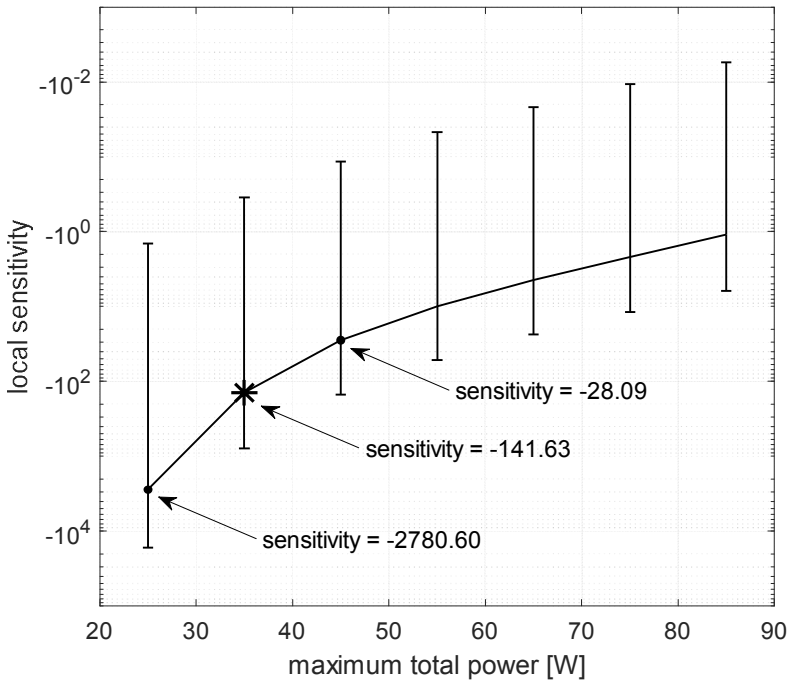

Figure 11. Local sensitivity of the power-efficient SDN control link problem by changing maximum total power P_{ctrl}.

link problem by changing the maximum total power P_{ctrl} from 25 W to 85 W. Monte Carlo simulations take 100 iterations for the steady-state performance analysis and the error bars indicate the maximum and minimum values of local sensitivity which deviate from the mean (i.e., a confidence interval with 100 percent). Small values of local sensitivity indicate that the relaxation of the total power consumption greatly increases the per-satellite average of the expected latency (21). The local sensitivity of the problem increases greatly by increasing P_{ctrl}, with a concave trend. The concavity manifests the point of diminishing returns where the maximum total power efficiently decreases the local sensitivity. A gradient in the low P_{ctrl} region is steeper because the satellites served by gateways under bad weather or at a long distance cannot be provided power enough to reduce the average of the expected latency. Hence by exploiting the diminishing marginal returns of the local sensitivity, we indicate P_{ctrl} equal to 35 W as the point of diminishing returns. In detail, local sensitivity dramatically increases from -2780.60 to -141.63 as P_{ctrl} increases from 25 to 35 W. However, local sensitivity increases smaller from -141.63 to -28.09 as P_{ctrl} increases from 35 W to 45 W, above the point of diminishing returns. Thus, from the local sensitivity analysis, a proper value of the maximum total power is suggested at 45-55 W, which is above the point of diminishing returns (35 W).

Fig. 12 shows the convergence of the daily average of $\mathbb{E}[\delta_s]$ of the power-efficient algorithm toward that of the ELM algorithm, by changing the maximum amount of total power P_{ctrl}. Monte Carlo simulations take 100 iterations for the steady-state performance analysis and 100 percent confidence intervals are given as error bars. Since the ELM algorithm is independent of P_{ctrl}, the average latency is presented as a constant. Although the average latency of the two algorithm do not make a large difference on the whole P_{ctrl} region, the daily average of $\mathbb{E}[\delta_s]$ of the proposed algorithm converges quickly to that of ELM as P_{ctrl} increases. In addition, the time averages of $\mathbb{E}[\delta_s]$ of the proposed algorithm and ELM are almost the same when P_{ctrl} is larger than 45 W while the control framework with the proposed algorithm uses much less power than that with ELM algorithm, which presents the power efficiency of the proposed algorithm. Interestingly, similar to the sensitivity analysis, the stability

analysis also suggests the point of diminishing return at 35 W. Hence, the management plane should set the maximum total power at 45-55 W above the point.

In addition, as maximum total power P_{ctrl} becomes smaller, the deviation of local sensitivity in Fig. 12 and the daily average of $\mathbb{E}[\delta_s]$ in Fig. 12 of the power-efficient algorithm becomes much larger. The reason can be found in the lack of the absolute total power consumption limited by P_{ctrl}. Under the condition that many gateways are in bad weather conditions or many satellites are at a long distance from gateways, the absolute amount of the total power is insufficient to provide enough power to all the satellites. This inconsistency problem of the proposed algorithm causes a large deviation as P_{ctrl} gets smaller. Fortunately, the deviations of both local sensitivity and the daily average of $\mathbb{E}[\delta_s]$ drastically decrease above the point of diminishing returns. Accordingly, for constructing both stable and consistent networks, P_{ctrl} should be set as 45-55 W, which is above the point of diminishing returns.

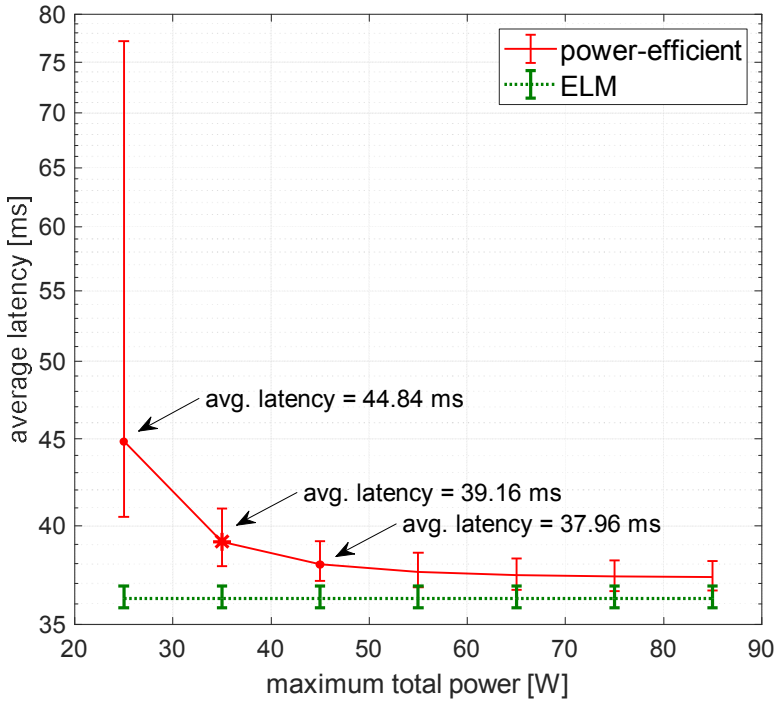

Figure 12. Average latency of ELM and power-efficient algorithms by changing maximum total power P_{ctrl}.

5. CONCLUSION

In this paper, for reliable and low latency control link association, we analyzed the expected latency metric from the perspective of multilayers and formulated the power-efficient SDN control link problem. The power-efficient control link problem exploits maximum total power P_{ctrl}, which utilizes the centralized property of the control plane. Based on the power control analysis derived from the problem, the power-efficient SDN control link algorithm has been proposed. The key point of the proposed algorithm is to decouple link association and power allocation, given the cross layer parameter $\left.\frac{\partial L_{gs}}{\partial P_g}\right|_{P_g=P_0}$.

In numerical results, the performance of the algorithm was analyzed in detail and we demonstrated the feasibility of the software-defined LEO satellite network. For the stability of the algorithm, further analysis on local sensitivity and stability was conducted to select the appropriate P_{ctrl} at the management plane. The management plane should select P_{ctrl} of the proposed algorithm above the point of diminishing marginal returns.

This study can be extended to various future work by presenting and solving problems that have not been discussed previously. We assume that the multi-controller system maintains coherence through east/westbound API. However, a large-scale and coherent control plane can be realized by full analysis on operating cost, synchronization cost, and latency of the controller network, which is left for the future work. In addition, future work may include the dynamic placement of VNFs on the satellite network and the comprehensive optimization of the Medium Access Control (MAC) layer, the Network layer and the Transport layer. Further analysis on the coherent control plane and VNF placement in the sky will blueprint the provision of various applications through the software-defined satellite network.

Appendix

The second derivative of expected latency L_{gs} with respect to transmit power P_g is given as

$$\frac{\partial^2 L_{gs}}{\partial P_g^2} = \left\{ \frac{2\left(\frac{m\gamma_{th}}{\overline{\gamma_{gc}}}\right)^m}{\Gamma\left(m, \frac{m\gamma_{th}}{\overline{\gamma_{gc}}}\right)} e^{-\frac{m\gamma_{th}}{\overline{\gamma_{gc}}}} + m + 1 - \frac{m\gamma_{th}}{\overline{\gamma_{gc}}} \right\} \times \left(\frac{1}{P_g \cdot \Gamma\left(m, \frac{m\gamma_{th}}{\overline{\gamma_{gc}}}\right)} \right)^2 \cdot \left(\frac{m\gamma_{th}}{\overline{\gamma_{gc}}}\right)^m \cdot e^{-\frac{m\gamma_{th}}{\overline{\gamma_{gc}}}}, \quad (27)$$

where the term after the multiplication sign $\times$ is positive because the average SNR $\overline{\gamma_{gc}}$ and other parameters are always positive. Accordingly, the expected latency L_{gs} is convex with respect to transmit power P_g if

$$\frac{2\left(\frac{m\gamma_{th}}{\overline{\gamma_{gc}}}\right)^m}{\Gamma\left(m, \frac{m\gamma_{th}}{\overline{\gamma_{gc}}}\right)} e^{-\frac{m\gamma_{th}}{\overline{\gamma_{gc}}}} > \frac{m\gamma_{th}}{\overline{\gamma_{gc}}} - (m+1). \quad (28)$$

Let $x = \frac{\gamma_{th}}{\overline{\gamma_{gc}}}$ be the ratio of SNR threshold to average SNR. Then, the left side term $L(\overline{\gamma_{gc}})$ and the right side $R(\overline{\gamma_{gc}})$ of the inequality (28) can be written as functions of x, respectively:

$$L(x) = \frac{2(mx)^m}{\Gamma(m, mx)} e^{-mx}, \quad (29)$$

$$R(x) = mx - (m+1), \quad (30)$$

We claim that the expected latency is convex with respect to P_g under the condition that m is an integer by proving that $L(x) > R(x)$ for all x and integer $m \geq 1$.

1) If $mx < (m+1)$, it is trivial because $L(x)$ is positive for all x.

2) If $mx \geq (m+1)$, take the logarithm on both $L(x)$ and $R(x)$ and let the left side and right side

$L_1(x)$ and $R_1(x)$, respectively. Then each is written as

$$L_1(x) = \log \frac{2}{\Gamma(m, mx)} + m\log mx - mx, \tag{31}$$

$$R_1(x) = \log\{mx - (m+1)\}. \tag{32}$$

For integer m, we can rewrite the upper incomplete gamma function $\Gamma(m, mx)$ as $\sum_{i=0}^{m-1} \frac{d^i}{d(mx)^i}(mx)^{m-1} e^{-mx}$ [49]. Then, $L_1(x)$ is written again as

$$L_1(x) = \log 2 - \log \sum_{i=0}^{m-1} \frac{d^i}{d(mx)^i}(mx)^{m-1} + m \log mx. \tag{33}$$

Add $\log \sum_{i=0}^{m-1} \frac{d^i}{d(mx)^i}(mx)^{m-1}$ to both sides and let the left side be $L_2(x)$ and the right side be $R_2(x)$. Then $L_2(x)$ and $R_2(x)$ satisfy the following inequality:

$$\begin{aligned} R_2(x) &= \log\{(mx)^m - 2(mx)^{m-1} - 3(m-1)(mx)^{m-2} - \cdots - m(m-1)!\,(mx) \\ &\quad - (m+1)(m-1)!\} \\ &\leq \log(mx)^m \\ &< \log\{2(mx)^m\} = L_2(x). \end{aligned} \tag{34}$$

Accordingly, expected latency L_{gs} is convex with respect to P_g, where shape factor m is an integer equal to or greater than 1.

References

[1] I. F. Akyildiz, and A. Kak, "The Internet of Space Things/CubeSats: A ubiquitous cyber-physical system for the connected world," *Computer Networks*, vol. 150, pp. 134-149, Feb 2019.

[2] J. P. Choi, S. Chang, and V. W. S. Chan, "Cross-layer routing and scheduling for onboard processing satellites with phased array antenna," *IEEE Transactions on Wireless Communications*, vol. 16, no. 1, pp. 180-192, Jan 2017.

[3] J. Liu, Y. Shui, L. Zhao, Y. Cao, W. Sun, and N. Kato, "Joint placement of controllers and gateways in SDN-enabled 5G-satellite integrated network," *IEEE Journal on Selected Areas in Communications*, vol. 36, no. 2, pp. 221-232, Feb 2018.

[4] S. Xu, X. W. Wang, and M. Huang, "Software-defined next-generation satellite networks: Architecture, challenges, and solutions," *IEEE Access*, vol. 6, pp. 4027-4041, 2018.

[5] M. Kaminskiy, "CubeSat data analysis revision," Goddard Space Flight Center, Greenbelt, Maryland, Tech. Rep. GSFC/Code 371, Nov 2015.

[6] D. Kreutz, F. M. V. Ramos, P. E. Verissimo, C. E. Rothenberg, S. Azodolmolky, "Software-defined networking: A comprehensive survey," *Proceedings of the IEEE*, vol. 103, no. 1, pp. 14-76, Jan 2015

[7] R. Cohen, L. Lewin-Eytan, J. S. Naor, and D. Raz, "Near optimal placement of virtual network functions," *2015 IEEE Conference on Computer Communications (INFOCOM)*, IEEE, Apr 2015, pp. 1346-1354.

[8] Z. Tang, B. Zhao, W. Yu, Z. Feng, and C. Wu, "Software defined satellite networks: Benefits and challenges," *2014 IEEE Computers, Communications and IT Applications Conference*, IEEE, Oct 2014, pp. 127-132.

[9] B. Heller, R. Sherwood, and N. McKeown, "The controller placement problem," *Proceedings of the first workshop on Hot topics in software defined networks*, ACM, 2012, pp. 7-12.

[10] Y. Li, and M. Chen, "Software-defined network function virtualization: A survey," *IEEE Access*, vol. 3, pp. 2542-2553, 2015.

[11] J. Sherry, S. Hasan, C. Scott, A. Krishnamurthy, S. Ratnasamy, and V. Sekar, "Making middleboxes someone else's problem: network processing as a cloud service," *ACM SIGCOMM Computer Communication Review*, ACM, vol. 42, no. 4, pp. 13-24, 2012.

[12] "SDN architecture overview," White Paper, Open Networking Foundation, Dec 2013.

[13] H. Kim, and N. Feamster. "Improving network management with software defined networking," *IEEE Communications Magazine*, vol. 51, no.2, pp. 114-119, 2013.

[14] T. Rossi, M. D. Sanctis, E. Cianca, C. Fragale, M. Ruggieri, and H. Fenech, "Future space-based communications infrastructures based on high throughput satellites and software defined networking," *2015 IEEE International Symposium on Systems Engineering (ISSE)*, IEEE, Sep 2015, pp. 332-337.

[15] J. Zhang, X. Zhang, M. A. Imran, B. Evans, Y. Zhang, and W. Wang, "Energy efficient hybrid satellite terrestrial 5G networks with software defined features," *Journal of Communications and Networks*, vol.19, no. 2, pp. 147-161, Apr 2017.

[16] C. I. C. Rowell, S. Han, Z. Xu, G. Li, and Z. Pan, "Toward green and soft: A 5G perspective," *IEEE Communications Magazine*, vol. 52, no. 2, pp. 66-73, Feb 2014.

[17] P. Gandotra, R. K. Jha, and S. Jain, "Green communication in next generation cellular networks: A survey," *IEEE Access*, vol. 5, pp. 11727-11758, 2017.

[18] M. Werner, C. Delucchi, H. J. Vogel, G. Maral, and J. J. D. Ridder, "ATM-based routing in LEO/MEO satellite networks with intersatellite links," *IEEE Journal on Selected areas in Communications*, vol. 15, no. 1, pp. 69-82, Jan 1997.

[19] A. Donner, M. Berioli, and M. Werner, "MPLS-based satellite constellation networks," *IEEE Journal on Selected areas in Communications*, vol. 22, no. 3, pp. 438-448, Apr 2004.

[20] M. Werner, "A dynamic routing concept for ATM-based satellite personal communication networks," *IEEE journal on selected areas in communications*, vol. 15, no. 8, pp. 1636-1648, Oct 1997.

[21] L. Bertaux, S. Medjiah, P. Berthou, S. Abdellatif, A. Hakiri, P. Gelard, F. Planchou, and M. Bruyere, "Software defined networking and virtualization for broadband satellite networks," *IEEE Communications Magazine*, vol. 53, no. 3, pp. 54-60, Mar 2015.

[22] Z. Zhang, B. Zhao, W. Yu, and C. Wu, "Poster: An efficient control framework for supporting the future SDN/NFV-enabled satellite network," *Proceedings of the 23rd Annual International Conference on Mobile Computing and Networking*, ACM, 2017, pp. 603-605.

[23] X. Yu, W. Lei, L. Song, and W. Zhang, "A routing algorithm based on SDN for on-board switching networks," *Journal of Information Science and Engineering,* vol. 33, no. 5, 2017, pp. 1255-1266.

[24] Y. Zhu, L. Qian, L. Ding, F. Yang, C. Zhi, and T. Song, "Software defined routing algorithm in LEO satellite networks," *2017 International Conference on Electrical Engineering and Informatics (ICELTICs)*, IEEE, Oct 2017, pp. 257-262.

[25] P. Du, S. Nazari, J. Mena, R. Fan, M. Gerla, and R. Gupta, "Multipath TCP in SDN-enabled LEO satellite networks," *MILCOM 2016-2016 IEEE Military Communications Conference*, IEEE, Nov 2016, pp. 354-359.

[26] M. F. Bari, A. R. Roy, S. R. Chowdhury, Q. Zhang, M. F. Zhani, R. Ahmed, and R. Boutaba, "Dynamic controller provisioning in software defined networks," *Proceedings of the 9th International Conference on Network and Service Management (CNSM)*, Oct 2013, pp. 18-25.

[27] S. Lange, S. Gebert, T. Zinner, P. Tran-Gia, D. Hock, M. Jarschel, and M. Hoffmann, "Heuristic approaches to the controller placement problem in large scale SDN networks," *IEEE Transactions on Network and Service Management*, vol. 12, no. 1, pp. 4-17, Mar 2015.

[28] A. Papa, T. de Cola, P. Vizarreta, M. He, C. Mas Machuca, and W. Kellerer, "Dynamic SDN controller placement in a LEO constellation satellite network," *2018 IEEE Global Communications Conference (GLOBECOM)*, IEEE, 2018.

[29] M. Berioli, A. Molinaro, S. Morosi, and S. Scalise, "Aerospace communications for emergency applications," *Proceedings of the IEEE*, vol. 99, no. 11, pp. 1922-1938, Nov 2011.

[30] J. F. Kurose, "Computer networking: A top-down approach featuring the internet," 7/E, *Pearson Education India,* 2017.

[31] M. Luglio, M. Y. Sanadidi, M. Gerla, and J. Stepanek, "On-board satellite "split TCP" proxy," *IEEE Journal on Selected Areas in Communications*, vol. 22, no. 2, pp. 362-370, Feb 2004.

[32] C. S. R. Murthy, "Ad hoc wireless network: Architectures and protocols," Pearson Education India, 2004.

[33] A. Mehrnia, and H. Hashemi, "Mobile satellite propagation channel. Part 1-a comparative evaluation of current models," *Gateway to 21st Century Communications Village. VTC 1999-Fall. IEEE VTS 50th Vehicular Technology Conference (Cat. No. 99CH36324)*, vol. 5, Sep 1999, pp. 2775-2779.

[34] M. O. Hasna, and M. S. Alouini, "Outage probability of multihop transmission over Nakagami fading channels," *IEEE Communications Letters*, vol. 7, no. 5, pp. 216-218, May 2003.

[35] M. Abramowitz, and I. A. Stegun, "Handbook of mathematical functions: with formulas, graphs, and mathematical tables," vol. 55, *Dover publications*, New York, 1972.

[36] A. Goldsmith, "Wireless communications," *Cambridge university press*, 2005.

[37] D. Tse, and P. Viswanath, "Fundamentals of wireless communication," *Cambridge university press*, 2005.

[38] D. P. Bertsekas, and J. N. Tsitsiklis, "Intoduction to probability," *Athena Scientific*, 2002.

[39] S. Boyd, and L. Vandenberghe, "Convex optimization," *Cambridge university press*, 2004.

[40] J. Ordonez-Lucena, P. Ameigeiras, D. Lopez, J. J. Ramos-Munoz, J. Lorca, and J. Folgueira,

"Network slicing for 5G with SDN/NFV: Concepts, architectures, and challenges," *IEEE Communications Magazine*, vol. 55, no. 5, pp. 80-87, May 2017.

[41] R. Ferrús, H. Koumaras, O. Sallent, G. Agapiou, T. Rasheed, M. A. Kourtis, C. Boustie, P. Gelard, and T. Ahmed, "SDN/NFV-enabled satellite communications networks: Opportunities, scenarios and challenges," *Physical Communication*, vol. 18, pp. 95-112, 2016.

[42] J. P. Choi, and V. W. S. Chan, "Resource management for advanced transmission antenna satellites," *IEEE Transactions on Wireless Communications*, vol. 8, no. 3, pp. 1308-1321, Mar 2009.

[43] Y. Nesterov, and A. Nemirovskii, "Interior-point polynomial algorithms in convex programming," vol. 13, *Siam*, 1994.

[44] T. Dreischer, H. Kellermeier, E. Fishcer, and B. Wandernoth, "Advanced miniature optical terminal family for inter-satellite links in space communication networks," *Proc. 4th European Conf. Satellite Communications (ECSC 4)*, 1997, pp. 73-78.

[45] M. D. Kennedy, and P. L. Malet, "Application for authority to construct, launch and operate the Celestri multimedia LEO system," *Filling to FCC*, 1997.

[46] S. R. Pratt, R. A. Raines, C. E. Fossa, and M. A. Temple, "An operational and performance overview of the IRIDIUM low earth orbit satellite system," *IEEE Communications Surveys*, vol. 2, no. 2, pp. 2-10, Second 1999.

[47] Globalstar satellite phone. Accessed: Aug. 7, 2019. [Online]. Available: https://www.pivotel.co.nz/pivotel_globalstar_international_coverage.

[48] "Enhanced network survivability performance," ANSI, New York, NY, USA, Tech. Rep. t1.tr.68-2001, 2001.

[49] U. Blahak, "Efficient approximation of the incomplete gamma function for use in cloud model applications," *Geoscientific model development*, vol. 3, no. 2, pp. 329-336, 2010.

요 약 문

소프트웨어 정의 LEO 위성 네트워크의 무선 제어 링크에 관한 연구

저궤도(LEO) 위성 네트워크는 데이터 전달 장치를 간소화하고 서비스 다양성을 향상시키는 등, 소프트웨어 정의 네트워킹(SDN)로부터 다양한 이점을 얻을 수 있다. 그러나 SDN 을 위성 네트워크에 적용하기 위해서는, 신뢰성 있는 SDN 제어 링크가 위성 게이트웨이로부터 위성까지 연결되어야 하며, 위성 네트워크의 무선 특성과 이동성이 동시에 고려되어야 한다. 이러한 특성들은 제어 링크 연결과 게이트웨이 전력 할당 모두에 영향을 미치기 때문에, 우리는 이러한 교차 계층 문제를 SDN 제어 링크 문제로 새롭게 정의한다. 이 문제는 전송 계층의 자동 재전송 요구(ARQ) 및 전송 제어 프로토콜(TCP), 네트워크 계층의 라우팅, 물리 계층의 전력 할당과 같은 다중 계층의 관점에서 논의된다. 본 논문에서는 제어 링크 설정에 필요한 게이트웨이 전력 효율을 높이기 위해 최대 총 전력을 제한하는 중앙집권화 SDN 제어 프레임워크를 도입한다. 제안된 문제에 대한 전력 할당 분석을 기반으로, 전력 소비가 적으면서도 지연이 적은 제어 링크를 연결하는 전력 효율적인 제어 링크 알고리즘이 제안된다. 제안된 제어 링크 알고리즘의 민감도 분석과 함께, 시뮬레이션 결과는 알고리즘에 의해 설정되는 제어 링크의 낮은 지연과 높은 신뢰성을 보여주며, 궁극적으로 소프트웨어 정의 LEO 위성 네트워크의 기술적 및 경제적 타당성을 제시한다.

핵심어: 소프트웨어 정의 위성 네트워크, 제어 링크, 교차 계층 최적화, 전력 효율 제어 링크 알고리즘.